Ultrafast Multipinhole SPECT Iterative Reconstruction Using CUDA-based GPU Computing

GTC 2012
San Jose, CA

F. Alhassen[1], J. D. Bowen[1], H. Kudrolli[2], B. Singh[2], R. G. Gould[1], V. V. Nagarkar[2], Y. Seo[1]
[1]Department of Radiology and Biomedical Imaging, University of California, San Francisco, San Francisco, CA, USA, fares.alhassen@ucsf.edu
[2]Radiation Monitoring Devices, Inc., Watertown, MA, USA

We have developed an ultrafast SIR method for multipinhole SPECT programmed in CUDA and tested using a high performance graphic processing unit. We show significant performance improvement in reconstruction using both computer-generated and experimental sinograms, demonstrating an up-to **fifty-fold** speed enhancement with **virtually the same accuracy** as the CPU-based SIR (with 0.15% normalized root mean square error).

Motivation

Why use GPUs for statistic iterative reconstructions (SIRs)? [1]

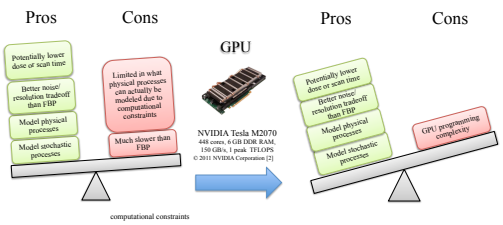

What's new here?

- GPU-based SIR for multipinhole SPECT using pre-computed system matrix
- Implemented using CUDA / CUSPARSE [3] GPU computing API
- Models finite pinhole apertures

Why multipinhole SPECT?

- High resolution with increased sensitivity compared to single pinhole or parallel hole SPECT
- Simultaneously acquired multiple views enhance accuracy in dynamic studies and reduce motion artifacts [2]

CPU vs. GPU Implementations

Hardware / Method	CPU	GPU
Processing cores	1 core of a AMD Opteron 6128 2.0 GHz CPU	448 cores of a NVIDIA Tesla M2070 GPU
RAM	16 GB	6 GB
Sparse matrix operations (projections)	Eigen 3.0 [4]	CUSPARSE 1.0 [5]
Rotation, correction, and reduction operations	C++ functions	CUDA kernels

Maximum-likelihood expectation maximization (MLEM)

MLEM SIR algorithm

Using matrix-based notation and implementation

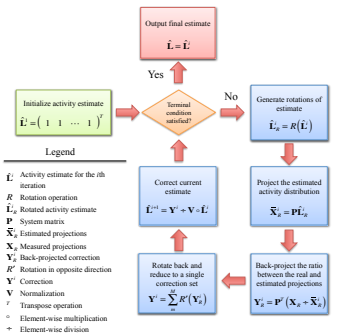

Ray-tracing

Incremental Siddon's Method [3]

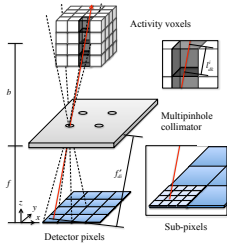

System matrix generation

Calculating weights between a pixel d and a voxel k through the ith pinhole

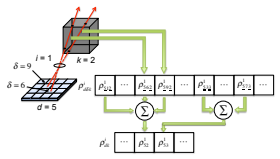

Ray tracing is faster on GPU

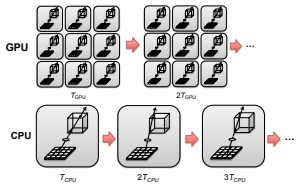

SIR Setup

Projections from digital phantoms

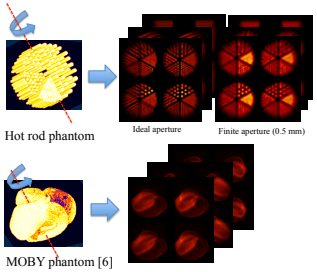

Projections from experimental acquisitions

With a microcolumnar scintillator [7]

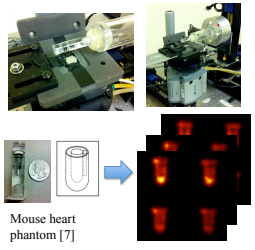

Reconstructions

Settings

Pinhole aperture	Phantom dimensions (voxels)	Sinogram dimensions (pixels)	Sub-pixels per pixel	Pinhole pixels per sub-pixel	Number of rays	System matrix size (MB)
Ideal	64^3	$256^2 \times 60$	3^2	1	589,824	76
Finite	64^3	$256^2 \times 60$	3^2	5^2	14,745,600	952-1072

Benchmarking

Pinhole aperture	Computational element	Ray tracing (s)	Average per iteration (s)	All iterations (s)	Total reconstruction (s)	GPU speed enhancement	NRMSE (%)
Ideal	CPU	6.31	10.26	513.20	527.05	37.25	0.15
	GPU	0.62	0.23	11.60	14.15		
Finite	CPU	197.68	47.3	2365.14	2586.02	47.71	1.24E-4
	GPU	13.30	0.78	38.86	51.20		
Finite (Mouse heart phantom)	CPU	356.47	60.79	3039.44	3421.37	37.25	4.50E-6
	GPU	23.11	0.83	41.28	66.47		

Reconstruction Accuracy

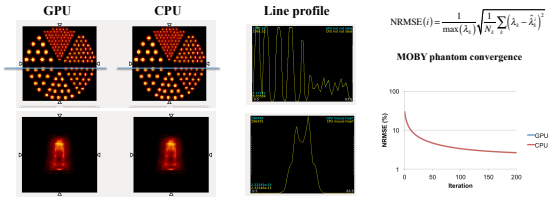

References

1. Pratx, G.; Chinn, G.; Olcott, P. D.; and Levin, C. S.; "Fast, Accurate and Shift-Varying Line Projections for Iterative Reconstruction Using the GPU," *Medical Imaging, IEEE Transactions on*, vol. 28, pp. 435-445, March 2009.
2. Xu, F.; "Fast Implementation of Iterative Reconstruction with Exact Ray-Driven Projector on GPUs," *Tsinghua Science & Technology*, vol. 15, pp. 30-35, 2010.
3. Han, G.; Liang, Z.; You, J.; , "A fast ray-tracing technique for TCT and ECT studies," Nuclear Science Symposium, 1999. Conference Record. 1999 IEEE, vol.3, no., pp.1515-1518 vol.3, 1999.
4. Eigen, http://eigen.tuxfamily.org/index.php?title=Main_Page, 2011.
5. Naumov, M.; "CUSPARSE Library: A Set of Basic Linear Algebra Subroutines for Sparse Matrices," GPU Technology Conference, 2070, Sept. 23, 2010.
6. Segars, W. P.; Tsui, B.M.W.; Frey, E. C.; Johnson, G. A.; and Berr, S. S.; Development of a 4D digital mouse phantom for molecular imaging research. *Molecular Imaging & Biology*, vol. 6, issue 3, p. 149-159, 2004.
7. Alhassen, F.; Kudrolli, H.; Singh, B.; Kim, S.; Seo, Y.; Gould R. G.; and Nagarkar, V. V.; "A preclinical SPECT camera with depth-of-interaction compensation using a focused-cut scintillator", Proc. SPIE 7961, 796121 (2011).